DEFENSE INFORMATION

This document contains information affecting the National Defense of the United States within the meaning of the Espionage Laws, Title 18, U.S.C., Section 793 and 794, the transmission or violation of which in any manner to an unauthorized person is prohibited by law.

BALTIMORE 3, MARYLAND

DISCLAIMER

THIS DOCUMENT CONSISTS OF 40 PAGES
NO 40 OF 100 COPIES, SERIES A

SUMMARY REPORT
AERODYNAMIC RE-ENTRY ANALYSIS
TASK 2 THERMOELECTRIC GENERATOR

MND-P-2291

Prepared by:

Robert Oehrli

Project Engineer
Douglas Harvey

LEGAL NOTICE

This report was prepared as an account of Government sponsored work. Neither the United States, nor the Commission, nor any person acting on behalf of the Commission:

A. Makes any warranty or representation, express or implied, with respect to the accuracy, completeness, or usefulness of the information contained in this report, or that the use of any information, apparatus, method, or process disclosed in this report may not infringe privately owned rights; or

B. Assumes any liabilities with respect to the use of, or for damages resulting from the use of any information, apparatus, method, or process disclosed in this report.

As used in the above, "person acting on behalf of the Commission" includes any employee or contractor of the Commission to the extent that such employee or contractor prepares, handles or distributes, or provides access to, any information pursuant to his employment or contract with the Commission.

DISTRIBUTION LIST

		Copy No.
1.	Air Force Ballistic Missile Division For: Major George Austin	1
2.	Air Research and Development Command Attn: RDTAPS, Capt. W. G. Alexander	2
3.	Army Ballistic Missile Agency Attn: ORDAB-c	3,4
4.	Atomic Energy Commission, Washington U.S. Atomic Energy Commission Attn: Mrs. J. M. O'Leary For: Lt. Col. G. M. Anderson, DRD Capt. John P. Wittry, DRD Lt. Col. Robert D. Cross, DRD R. G. Oehl, DRD Edward F. Miller, PROD Technical Reports Library	 5 6 7 8 9 10
5.	Atomics International Attn: Dr. Chauncey Starr For: J. Wetch	11
6.	Bureau of Aeronautics Attn: C. L. Gerhardt, NP	12
7.	Bureau of Ordnance Attn: Mrs. Maryle R. Schmidt or Laura G. Meyers (To be opened by addressee only) For: Ren SP	 13 14
8.	Bureau of Ships, Code 1500 Attn: Melvin L. Ball	15
9.	U.S. Atomic Energy Commission Canoga Park Area Office Attn: A. P. Pollman, Area Manager	16

DISTRIBUTION LIST (continued)

		Copy No.
10.	Chicago Operations Office U.S. Atomic Energy Commission Attn: A. I. Mylyck For: T. A. Nemzek Mr. Klein	17,18
11.	Chief of Naval Operations	19
12.	Department of the Army, Atomic Division	20
13.	Diamond Ordnance Fuse Laboratories Attn: ORDTL 06.33, Mrs. M. A. Hawkins	21,22,23
14.	Hanford Operations Office Attn: Technical Information Library	24
15.	Lockheed Aircraft Corporation Asst. AF Plant Representative For: John H. Carter	25,26
16.	Mound Laboratory Attn: Library and Records Center For: Mrs. Roberson	27
17.	National Advisory Committee for Aeronautics, Ames Attn: Smith J. De France, Director	28
18.	National Advisory Committee for Aeronautics, Langley Attn: Henry J. E. Reid, Director	29
19.	National Advisory Committee for Aeronautics Lewis Flight Propulsion Laboratory Attn: George Mandel	30
20.	Naval Ordnance Laboratory Attn: Eva Lieberman, Librarian	31,32,33
21.	Naval Research Laboratory, Code 1572 Attn: Mrs. Katherine H. Cass	34

DISTRIBUTION LIST (continued)

		Copy No.
22.	New York Operations Office U.S. Atomic Energy Commission Attn: Document Custodian	35,84
23.	Oak Ridge National Laboratory X-10, Laboratory Records Department Attn: Eugene Lamb	36
24.	Office of Naval Research, Code 735 Attn: E. E. Sullivan For: Code 429	37
25.	Project Rand Director, USAF Project Rand Attn: F. R. Collbohm For: Dr. John Huth	38
26.	Rome Air Development Center Attn: RCSG, J. L. Briggs	39
27.	Technical Information Service Extension U.S. Atomic Energy Commission Oak Ridge, Tennessee	40 through 64
28.	Thompson Ramo Wooldridge Staff Research and Development Attn: C. G. Martin	65,66,67
29.	University of California Radiation Laboratory Technical Information Division Attn: Clovis G. Craig For: Dr. Hayden Gordon	68
30.	Wright Air Development Center Attn: WCACT For: Capt. Clarence N. Munson, WCLPS G. W. Sherman, WCLEE WCOSI	69 70 71,72
31.	Jet Propulsion Laboratory Attn: W. H. Pickering, I. E. Newlan	73

DISTRIBUTION LIST (continued)

		Copy No.
32.	University of California Radiation Laboratory Technical Information Division Attn: Clovis G. Craig For: Dr. Robert H. Fox	74
33.	Los Alamos Scientific Laboratory Attn: Report Librarian For: Dr. George M. Crover	75
34.	Air Force Special Weapons Center Attn: Kathleen P. Nolan	76
35.	School of Aviation Medicine Randolph Air Force Base, Texas Attn: Col. J. E. Pickering	77
36.	Air Technical Intelligence Center Wright-Patterson Air Force Base, Ohio Attn: H. Holzbauer, AFCIN-4 Bla	78
37.	National Aeronautics and Space Administration Attn: Dr. Addison N. Rothrock	79 through 83

Addresses based on the latest edition of M-3679 as issued by the USAEC.

FOREWORD

This report has been prepared in compliance with Contract AT(30-1)-217. It summarizes the study conducted on aerodynamic re-entry analysis of the Task 2 thermoelectric generator.

CONTENTS

SUMMARY

An analytical trajectory and aerothermodynamic analysis of a satellite containing a Task 2 thermoelectric generator has been completed. A 300-statute mile circular polar orbit was used for this analysis and the launch was assumed to be from Vandenberg Air Force Base.

Results of this study show that upon natural decay from a successful mission, the radio-cerium fuel will burn up in space at high altitude, thus only a very minor amount of radio cerium will be released to the stratosphere.

A complete analyses of the fate of the radio-cerium fuel following various aborted launching attempts also has been carried out. Charts summarizing the various assumed failures and locations of the fuel following failure are shown.

A technical discussion of the methods used in performing the analysis is included in the report.

I. INTRODUCTION

To establish that a radioisotope fueled thermoelectric generator can be safely used in an orbital vehicle, all phases of the vehicle operation must be analyzed. One extremely critical phase occurs when a vehicle, near orbital velocity, re-enters the atmosphere. This could occur upon natural decay of the satellite from orbit or during an aborted final stage operation. One of the important aspects of this problem is the severe aerodynamic heating that the generator will undergo and its ultimate effect on the fate of the radio-cerium fuel. In addition, the location of the re-entering body is of importance when the possibility of release of even minute amounts of fuel is being considered.

The object of the present report is to analyze all possible re-entry conditions that might be imposed upon the Task 2 thermoelectric generator when used as a power supply for a typical satellite mission.

II. TECHNICAL DISCUSSION *

The following technical discussion involves calculating case histories of the radioisotope fueled unit during re-entry following a final stage failure while attempting to achieve a circular orbit. The problems of trajectory analysis, determination of aerodynamic heating and subsequent heat transfer including generator melting and/or oxidation are involved.

A. FINAL STAGE SATELLITE

A typical satellite installed in a launching vehicle is shown in Fig. 1. For the purpose of this study, the satellite is assumed to be entering a circular orbit at an altitude of 300 statute miles. The launch is from Vandenburg Air Force Base (VAFB) and is to establish a southerly polar orbit. At the end of the boost, and immediately before firing the injection stage, the characteristics of the satellite are:

Flight Altitude	
γ, Flight path angle--degrees	2
h, Altitude--feet	1,524,000
V, Velocity--feet/second	17,781
λ, Longitude--degrees West	121.67
ϕ, Latitude--degrees North	16.37
Physical Characteristics	
W_I, Initial weight--pounds	11,600
W_F, Fuel weight--pounds	6,640
I_{SP}, Specific impulse--seconds	266.43
t_b, Burning time--seconds	106.40

* Trajectory Analysis--W. Hagis
Aerodynamic Heating Analysis--C. Milewski

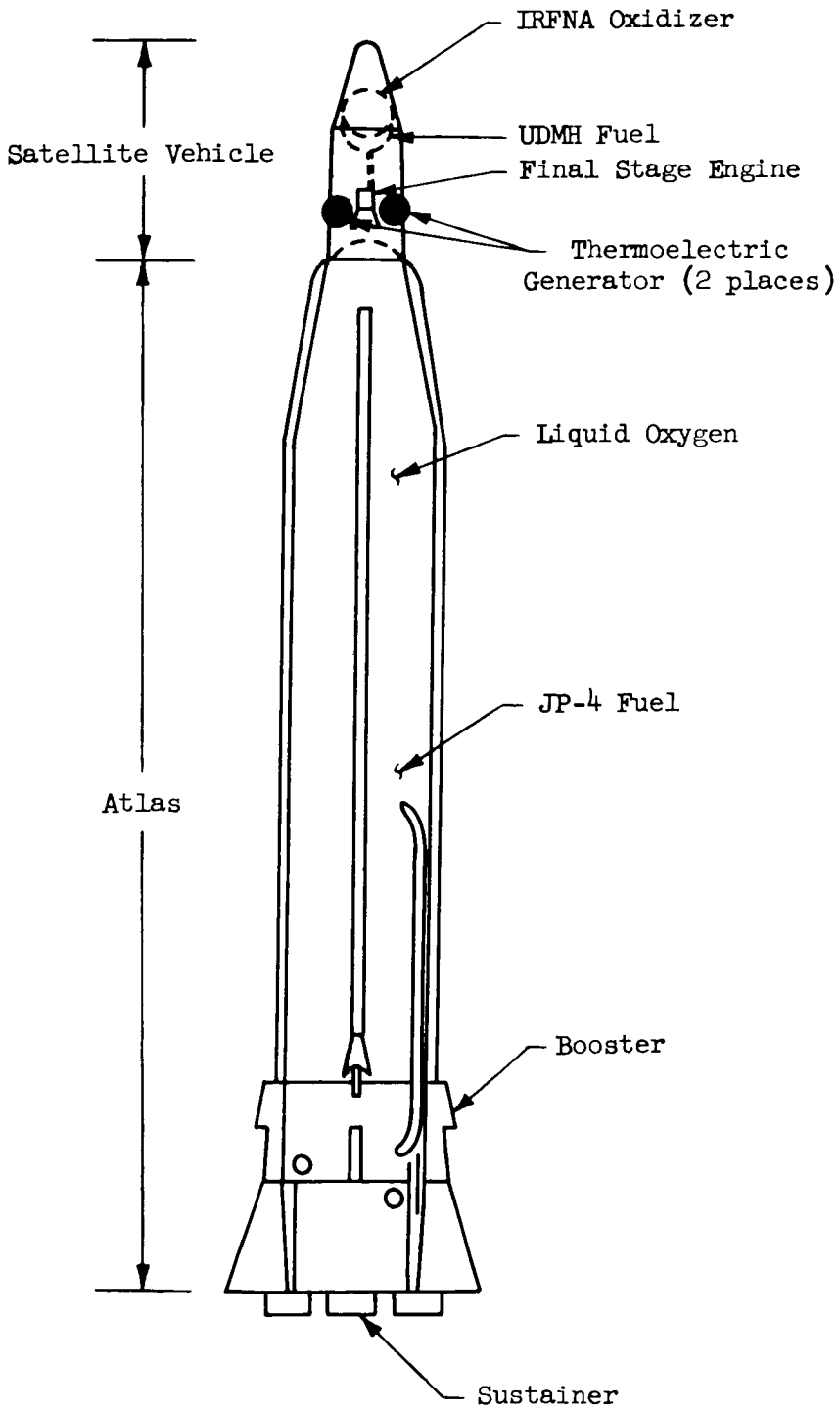

Fig. 1. Typical Vehicle Configuration

B. THERMOELECTRIC GENERATOR

The detailed configuration of the Task 2 generator is shown in Fig. 2. The fuel is a Cerium-144-loaded assembly shown as Configuration A in Fig. 3. The heavy inner construction has been devised to withstand terminal velocity impacts. The material for this core is a super alloy such as Inconel Hastelloy. Lead telluride thermoelectric elements are mounted between thin concentric outer shells as shown in Fig. 2. The inner wall of the outer shell is stainless steel and is supported with a stainless steel truss structure as shown in Fig. 4.

C. CALCULATION PROCEDURE

The scheme for the analytical procedure carried out in this report is presented in Fig. 5. Essentially, the final stage is ignited at such an altitude and flight condition that if the stage fires successfully, the satellite would enter a 300-mile circular polar orbit. If the thrust is prematurely cut off or misaligned during this stage of injection, an undesirable flight altitude will be obtained. Depending upon the degree of error, the satellite will enter into an elliptical orbit or immediately re-enter the atmosphere. The case history of the thermoelectric generator then becomes of concern. In particular, the location and condition of the isotopic fuel and its containment must be determined. Figure 5 illustrates a case where the satellite does not go into orbit, but re-enters the atmosphere due to a premature thrust cutoff. Aerodynamic forces become significant at an altitude near 375,000 feet and the thin outer shell of the satellite vehicle will fail. As the isotope unit with some structural aluminum attached is released, the aluminum outer wall and steel inner wall of the generator shell are subsequently melted and the core is exposed to the atmosphere. The fuel core then finally melts and burns up at altitude. A change in ballistic coefficient between the less dense complete unit and heavier core is noted. For purposes of determining final terminal velocities, these ballistic coefficient values are increased when the velocity becomes subsonic.

1. Program

The burning time for the final powered stage of the satellite injection is given as 106.4 seconds. Thrust cutoffs were assumed to occur at times of 21.5, 58.8, 85.6, 100.8 and 103.4 seconds. These values correspond to velocity increments (ΔV) of 6000, 4000, 2000, 600 and 400 feet per second less than the velocity required to achieve a circular orbit at 300 statute miles.

In addition, at each of these times the engine axis of thrust was assumed to tilt 5, 45 and 90 degrees in pitch and yaw with no thrust cutoff. The history of the unit was calculated for each of these cases.

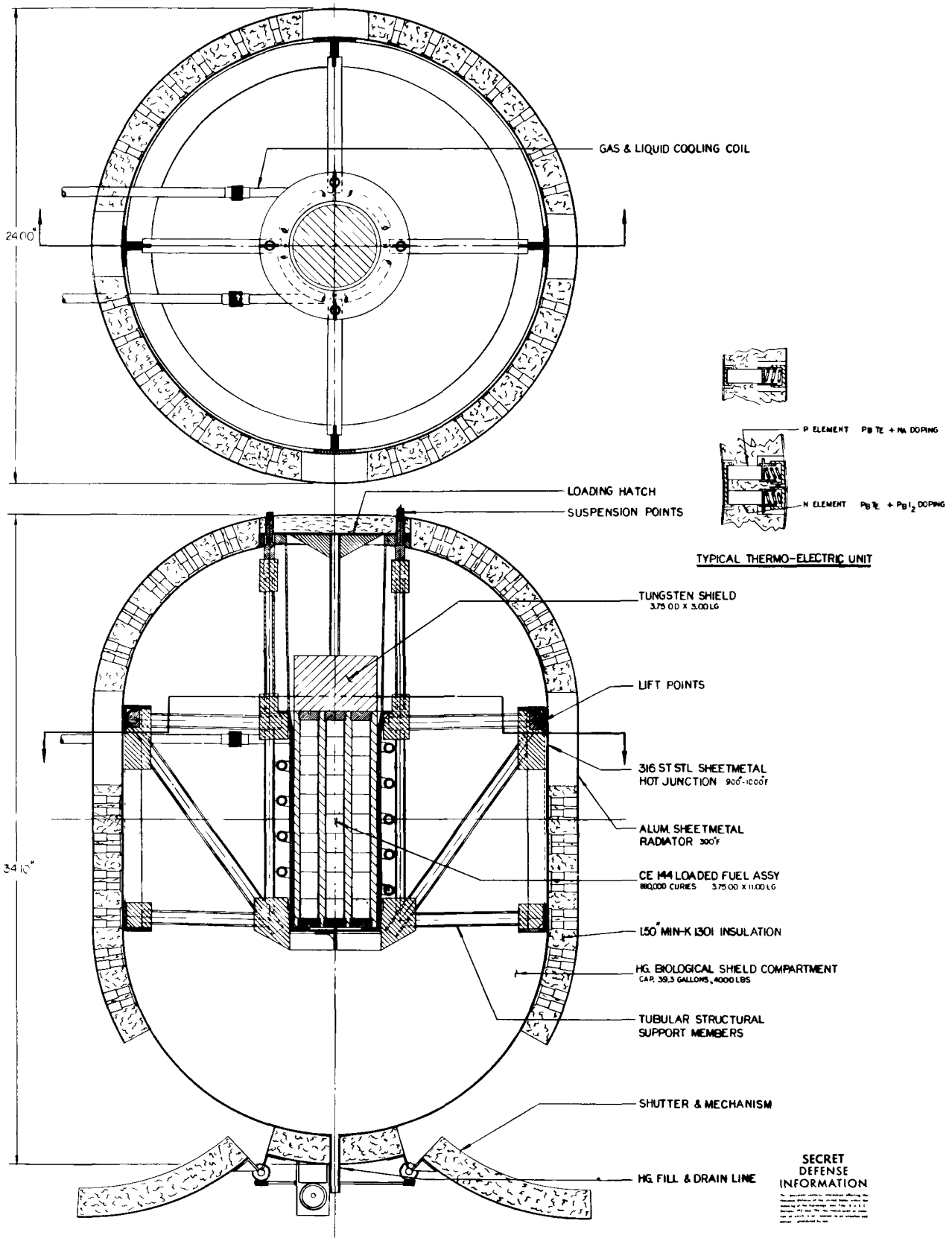

Fig. 2. Thermoelectric Generator

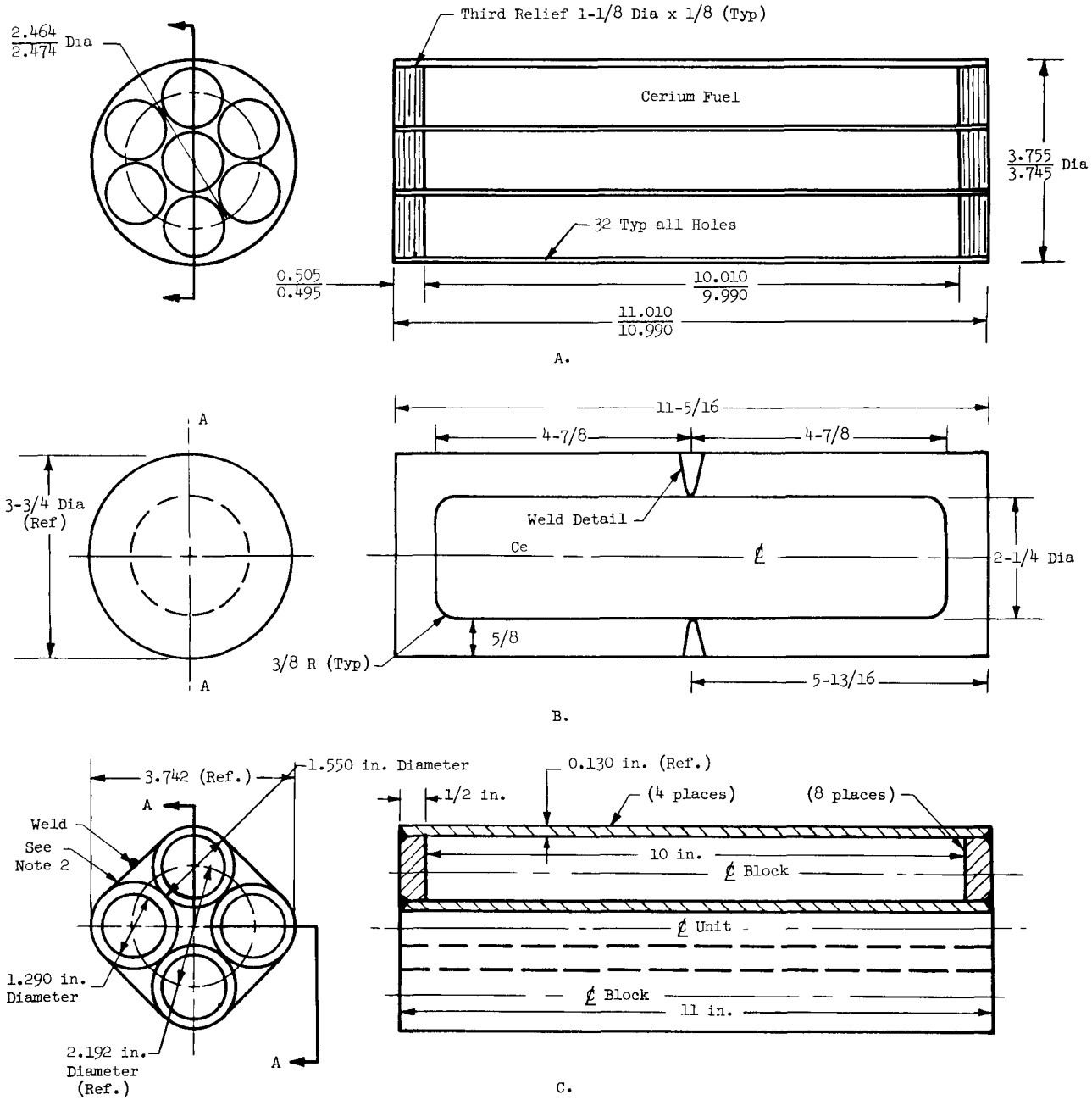

Fig. 3. Fuel Capsule Configurations

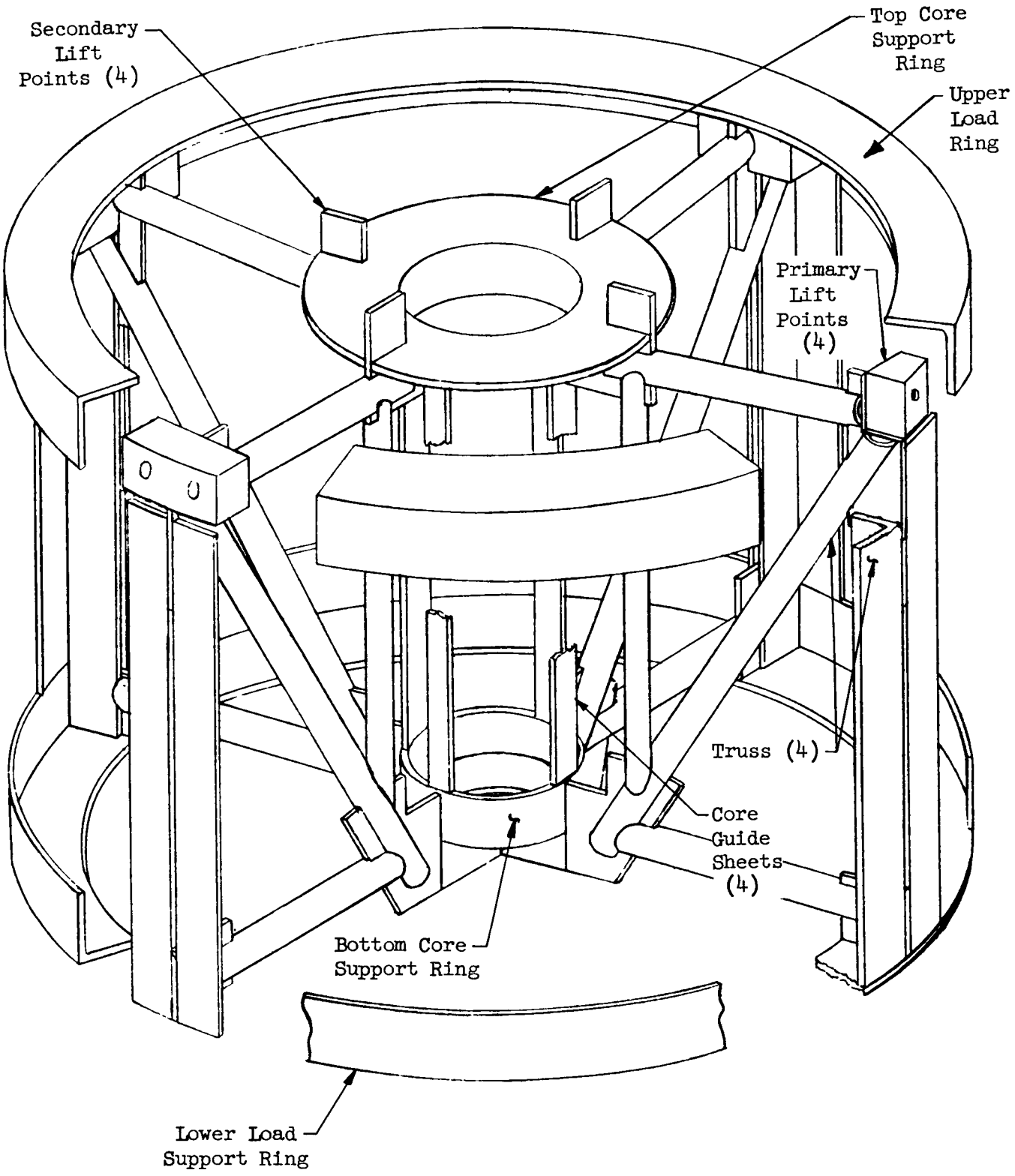

Fig. 4. Generator Truss Support Structure

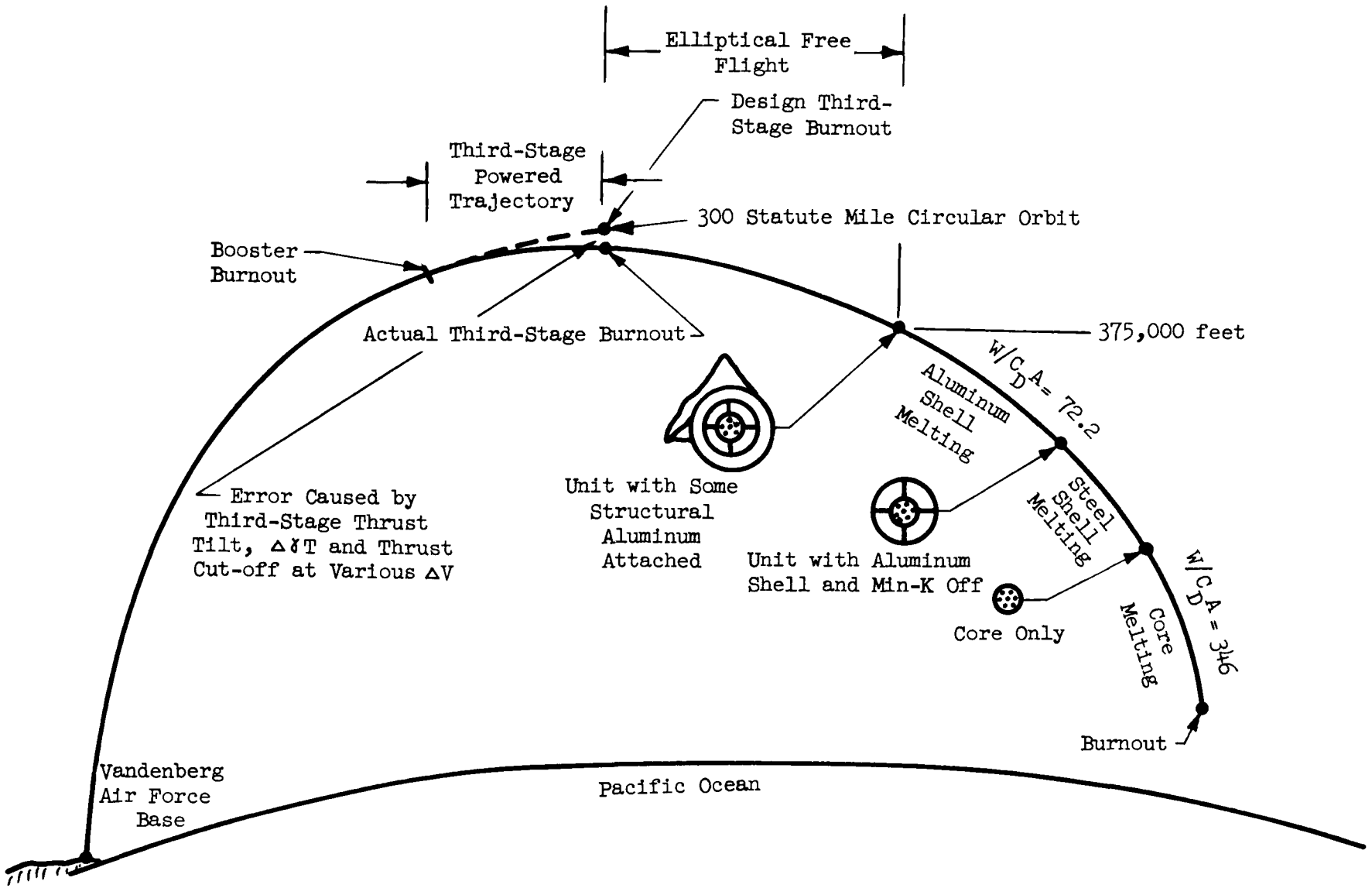

Fig. 5. Steps of Analytical Procedure

Further, re-entries for thrust cutoffs during various portions of the booster stage were also investigated.

Methods used for this analysis are described.

2. Trajectory Analysis

For the thrust cutoff and pitch program, a general N stage two-dimensional powered trajectory was used. In this case, zero lift powered phases were used. Where power or aerodynamic effects were predominate, the trajectory was integrated; when these conditions did not exist an elliptic path was used. Details of this method are presented in Ref. 1. The basic equations for integration are shown in Fig. 6.

The three-dimensional equations used to determine re-entry trajectories caused by thrust misalignments in yaw become somewhat more complicated and are not presented here. (These are reported in Refs. 2 and 3.) Typical trajectories obtained from these calculations are shown in Figs. 7, 8 and 9.

3. Aerodynamic Heating

On a blunt nose the aerodynamic heating becomes a function of nose shape, Mach number, atmospheric pressure and nose radius. The relations used are shown in Fig. 10.

For the present shell analysis, the laminar hemispherical values were used. An integration of the value around the entire nose indicates that an average value of 0.35 of the stagnation value would be applicable for the tumbling outer sphere. This method is somewhat conservative since no turblent flow heating was used. (Figure 10 shows that a considerable amount of heating could be derived from this source.) In general, on a roughened spherical nose, turbulent flow will be obtained back of the 40-degree total central arc.

For the round cylindrical core analysis, the two-dimensional equivalent of K_1 and K_3 must be used. These are shown on Fig. 10.

Figure 11 shows a typical re-entry heating rate.

4. Heat Transfer

With the trajectory and aerodynamic heating methods established it becomes necessary to calculate the heat transfer through the unit.

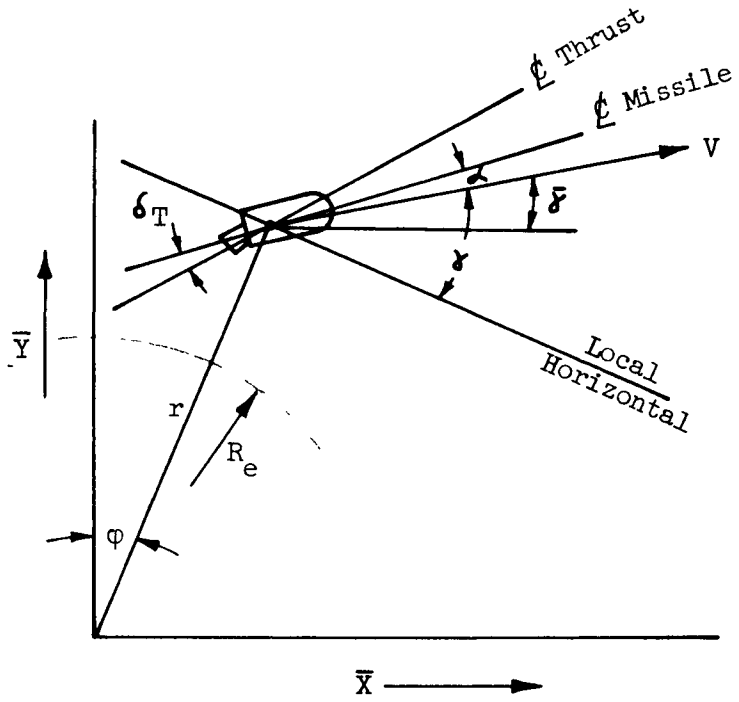

$\bar{X}$, $\bar{Y}$	Inertial axis
R_e	Radius of earth
r	Radius of vehicle from center of earth
φ	Range angle
α	Vehicle angle of attack
γ	Local flight path angle
$\bar{\gamma}$	Inertial flight path angle
δ_p	Thrust alignment in pitch
μ	Earths gravitational constant
m	Mass of vehicle

Equations

$$\ddot{\bar{X}} = -\left[\frac{T \sin(\alpha + \delta_p) + L}{m} - \frac{\mu}{r^2}\cos\bar{\gamma}\right]\sin\bar{\gamma} + \left[\frac{T\cos(\alpha+\delta_p) - D}{m} - \frac{\mu}{r^2}\sin\gamma\right]\cos\bar{\gamma}$$

$$\ddot{\bar{Y}} = \left[\frac{T \sin(\alpha + \delta_p) + L}{m} - \frac{\mu}{r^2}\cos\bar{\gamma}\right]\cos\bar{\gamma} + \left[\frac{T\cos(\alpha+\delta_p) - D}{m} - \frac{\mu}{r^2}\sin\gamma\right]\sin\bar{\gamma}$$

Fig. 6. Basic Two-Dimensional Trajectory Equations

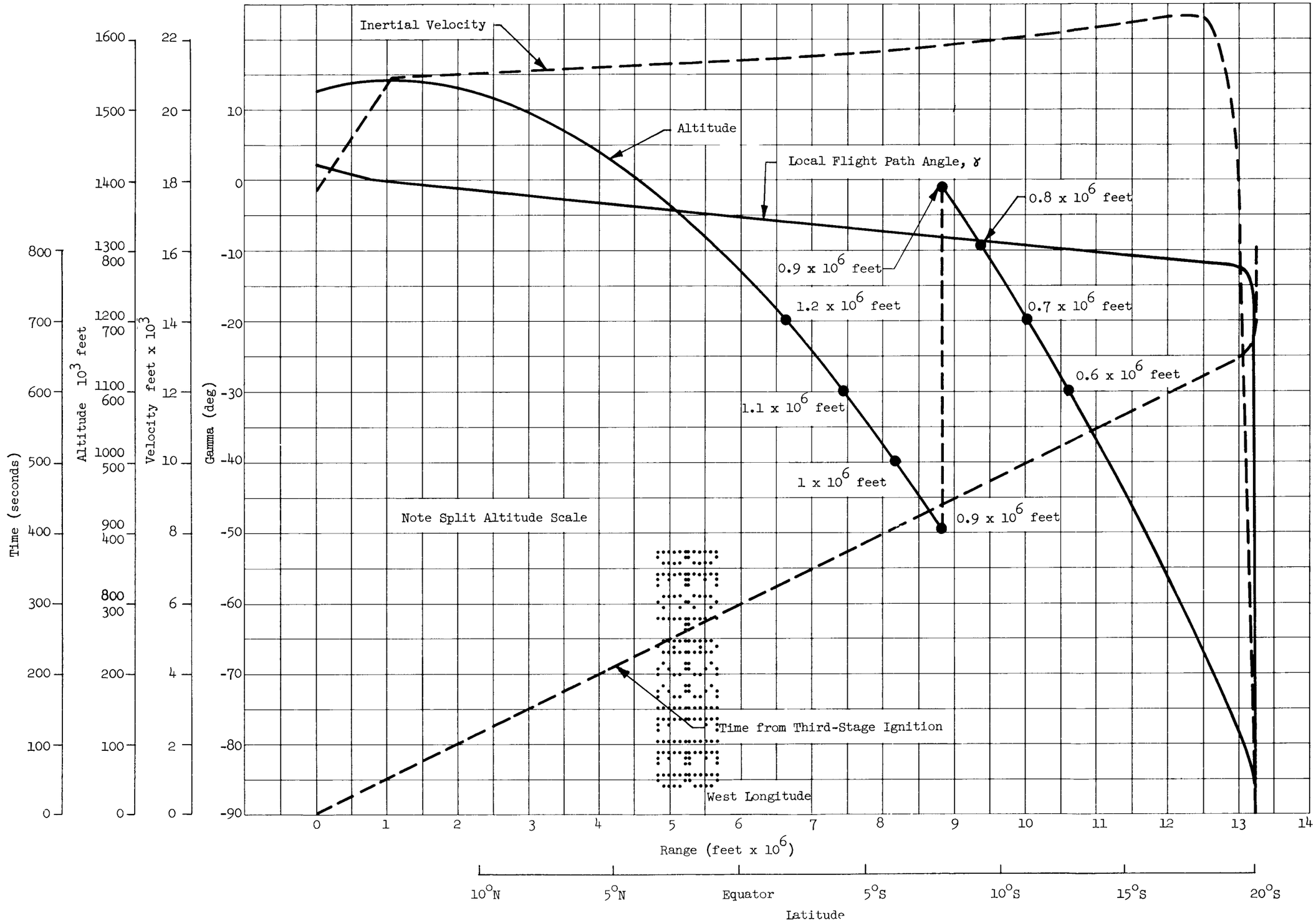

Fig. 7. Trajectory 5D Aerodynamic Data as Function of Range from Third-Stage Ignition

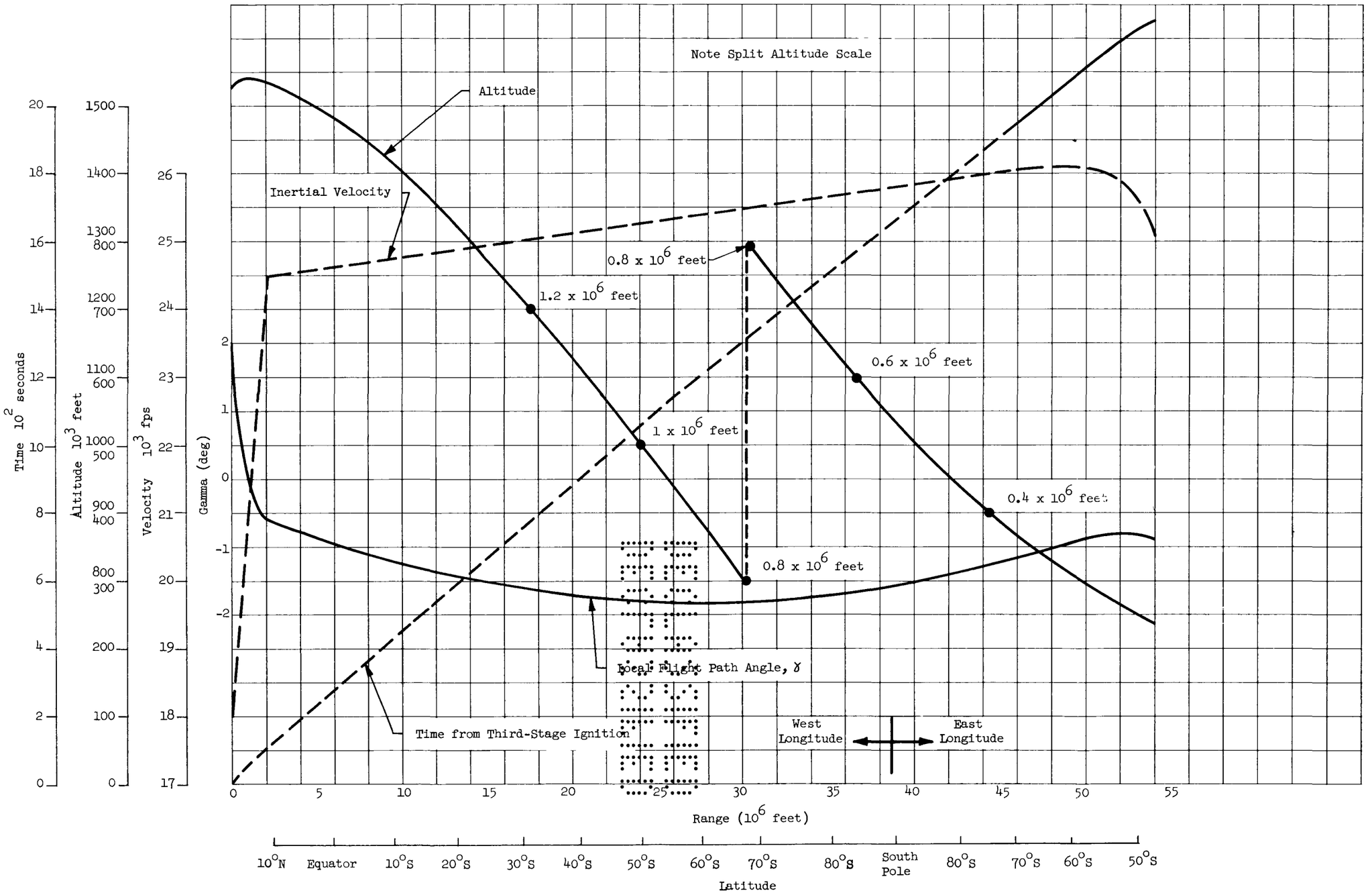

Fig. 8. Trajectory 5A Aerodynamic Data as Function of Range from Third-Stage Ignition

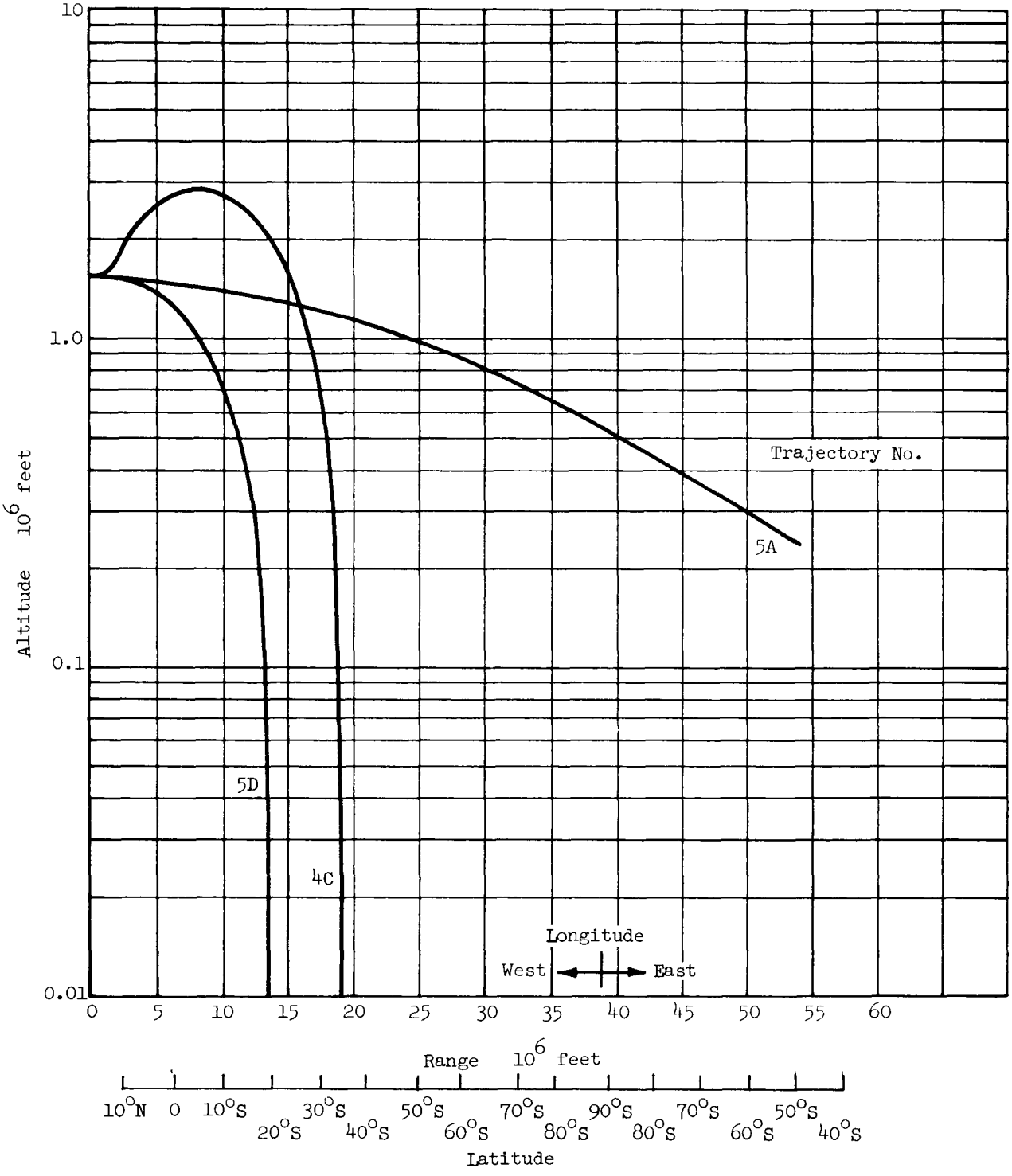

Fig. 9. Re-Entry Altitude as Function of Range from Third Stage Ignition

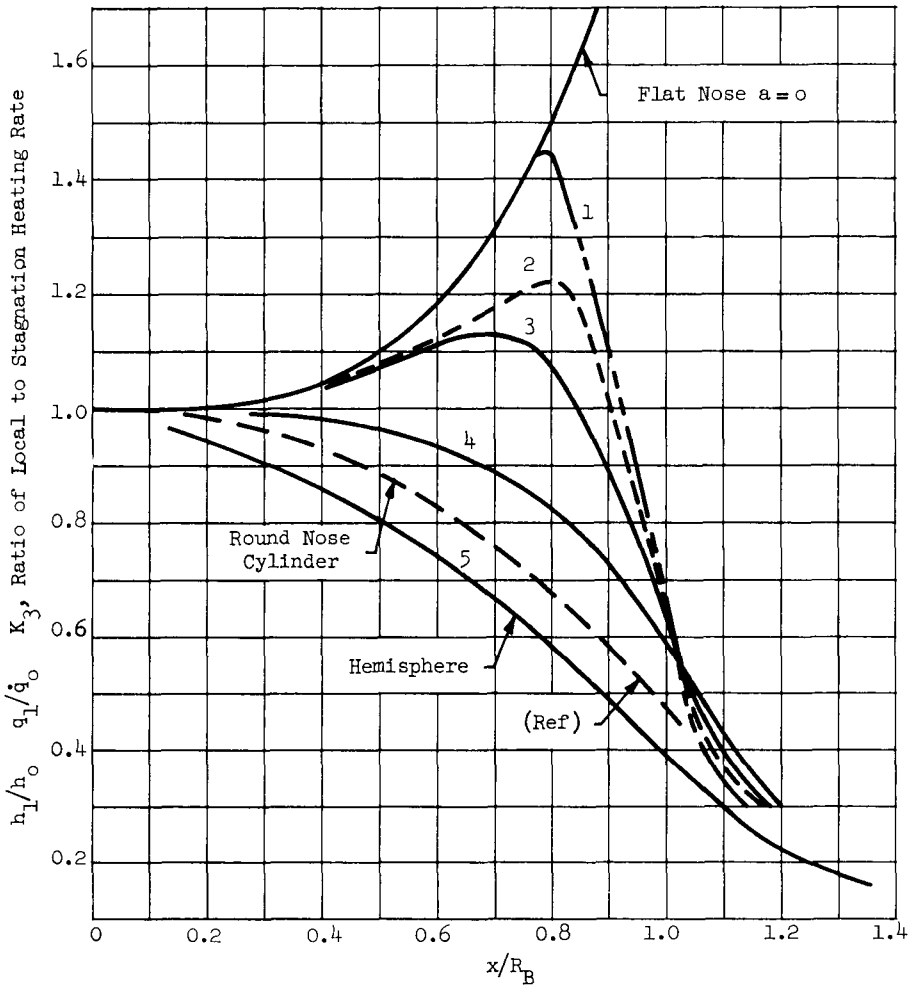

$$\frac{z^2}{a^2} + y^2 = R_B^2$$

1 a = 0.007
2 a = 0.333
3 a = 0.5
4 a = 0.666
5 a = 1.0

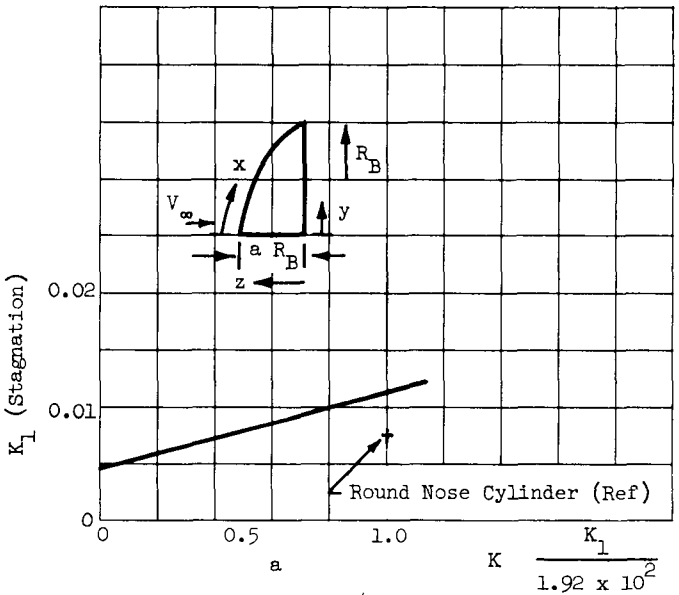

$$h_1 = K K_3 M_\infty^{1.34} T_\infty^{0.17} \left(\frac{P_\infty}{R_B}\right)^{1/2} \left[1 - 0.0137 M_\infty\right] \text{ Btu/sq ft-sec } ^\circ F$$

$$\dot{q}_1 = K_1 K_3 M_\infty^{3.34} \left(\frac{P_\infty}{R_B}\right)^{1/2} \left[1 - 0.0137 M_\infty\right] \text{ Btu/sq ft-sec}$$

$$\dot{q}_T/\dot{q}_1 = 1.19 K_3^{0.6} \left(\frac{P_\infty}{2R_B}\right)^{0.3} \times \left[1 + 0.0096 M_\infty\right]^{0.6}$$

Fig. 10. Axially Symmetric Nose Aerodynamic Heating

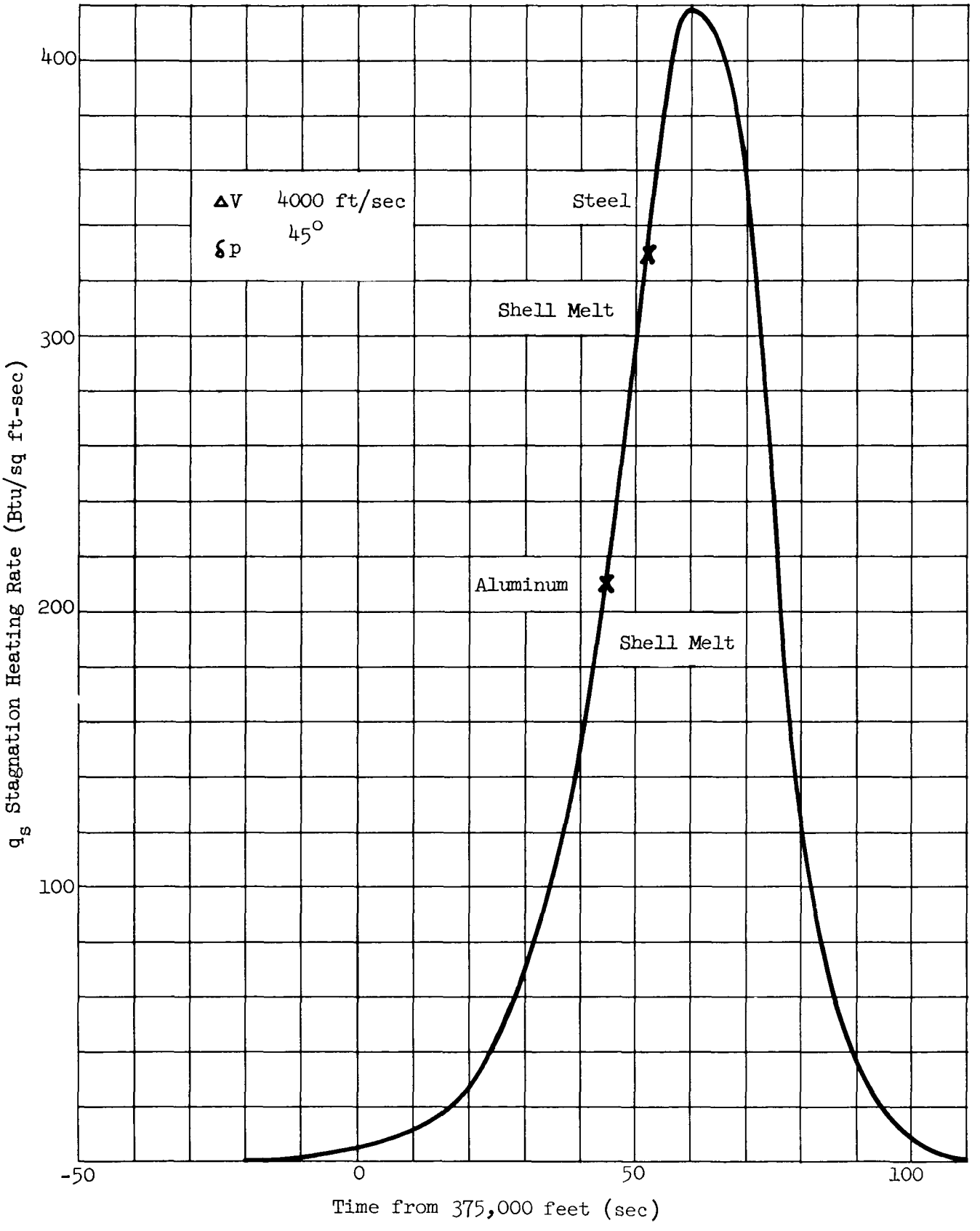

Fig. 11. Shell Stagnation Heating Rate

First, an equivalent heat transfer configuration for the basic thermoelectric generator was established and is shown here.

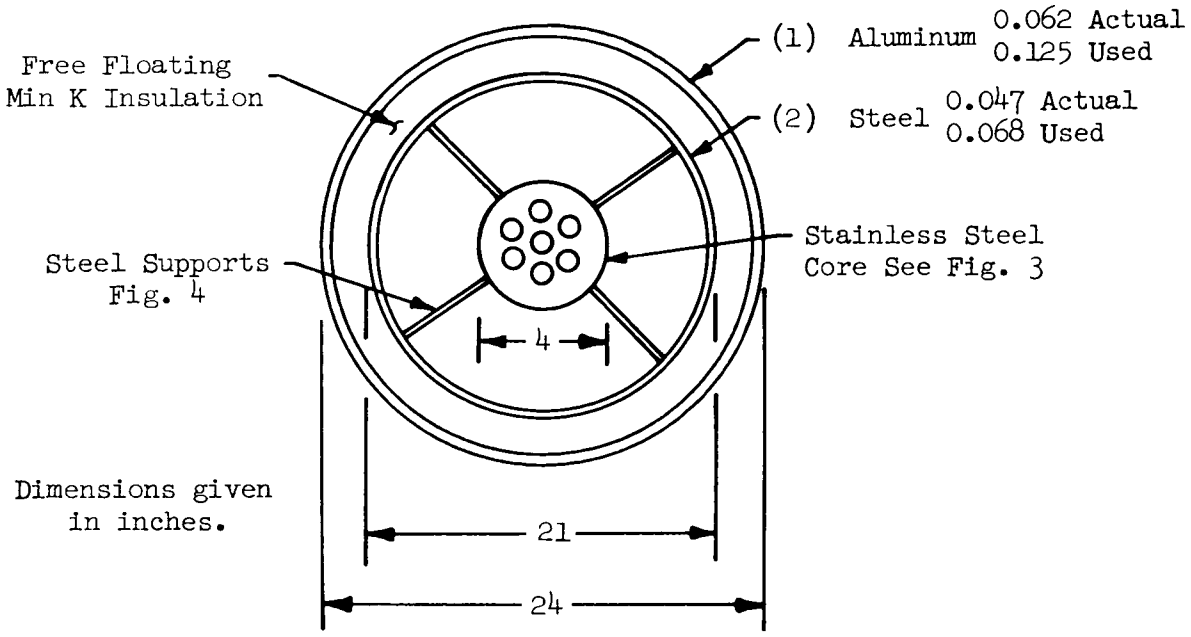

(1) To represent the effect of light aluminum satellite structure, the outer shell of the generator was increased to 0.125 from the actual value of 0.0625.

(2) An additional five pounds of steel were distributed both to the outer steel shell and the stainless core. The five pounds represent 1/6 of the support structure weight. This increased the stainless steel shell from the actual value of 0.047 to 0.068 and the core diameter from 3.75 to 4.0 inches.

The following material properties were used.

Outer Shell	Aluminum	Steel
C_p, Specific heat--Btu/lb ^{o}F	0.226	0.150
T_m, Melting temperature--^{o}R	1670	3000
L_F, Heat of fission--Btu/lb	167	117
ρ, Density--lb/cu ft	169	496

Core

Since the heating elements are already molten, it is assumed that this liquid has no effect on the heat balance and serves only to maintain shape.

C_p = 0.105 at 100° F
0.120 at 1000° F

*K = 3.3 at 100° F
6.35 at 1000° F

T_m = 3000° R

L_F = 117 Btu/lb

*ρ = 0.126 lb/cu in.

Using this information and heat input data from curves similar to Fig. 11, the heat balance equation for a number of elements may be calculated as shown in Fig. 12. The method illustrated in Fig. 12 is reported in Ref. 4.

To further illustrate the use of the method, consider the outer shell with its thin walls.

For the outer aluminum shell,

Heat In - Heat Radiated = Heat Stored + Phase Change

$$(\dot{q}_{in} - \sigma\epsilon T_w^4)\,\Delta t = W\,C_p\,\Delta T + L_F\,W$$

$$= W\,C_p\left(\Delta T + \frac{L_F}{C_p}\right)$$

For a time increment, Δt, the temperature increases an amount ΔT. The heat of fusion is equivalent to a temperature increase L_F/C_p. The material of a thin element can therefore be considered to be removed at $T = T_{melt} + L_F/C_p$. For aluminum, T_{melt} is 1670° R and the radiation is small.

* Forty-four percent of the core volume is steel, hence **K** = 0.44 K steel and ρ = 0.44 ρ steel.

Element	Aerodynamic Heat In	- Heat Radiated Out	+ Heat Conducted In -Out	= Heat Stored + Phase Change
①	$\dot{q}_{in}$	$- \sigma\epsilon \left(T_1^4 - T_\infty^4\right)$	$- \frac{k}{\Delta x}(T_1 - T_2)$	$= \frac{\rho C_p \Delta x}{\Delta t} \Delta T_1 + \frac{\rho \Delta x}{\Delta t} L_F = \frac{\rho C_p \Delta x}{\Delta t}\left(\Delta T_1 + \frac{L_F}{C_p}\right)$
②			$+ \frac{k}{\Delta x}(T_1 - T_2) - \frac{k}{\Delta x}(T_2 - T_3)$	$= \frac{\rho C_p \Delta x}{\Delta t} (\Delta T_2)$
③			$+ \frac{k}{\Delta x}(T_2 - T_3) - \frac{k}{\Delta x}(T_3 - T_4)$	$= \frac{\rho C_p \Delta x}{\Delta t} (\Delta T_3)$

etc.

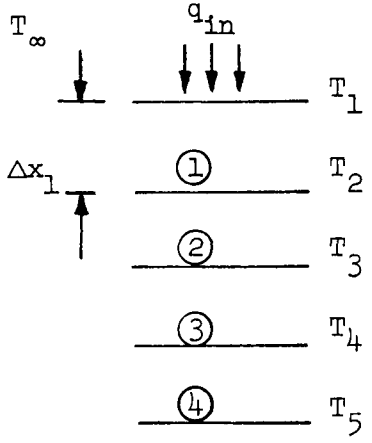

ΔT_1 = increment of temperature T_1 for a time increment Δt

For initial values of T_1, T_2 etc. a step by step solution of a series of set of simultaneous equation is performed. T_1 increases until $T_1 = T_{melt}$ at this time the heat balance (T_2, T_3 etc.) is held until T_1 increases an amount L_F/C_p. At this time the outer element ① is melted and the old element ② now becomes new element ① and the process is repeated. For a sphere or cylinder, the heating rate is increased for a decrease in radius.

Fig. 12. Heat Transfer Scheme (Per Unit Area)

$$\dot{q}_{in} A = \frac{\rho A \Delta x}{\Delta t} \Delta T$$

$$\Delta T = \frac{\dot{q}_{in}}{\rho \Delta x C_p} \Delta t$$

Δx, Shell thickness--feet 0.0104

Δt, Time increment--seconds 10

$\dot{q}_{in}$, 0.35 stagnation heating rate Fig. 11

$$T_{final} = T_m + \frac{L_F}{C_p} = 1670 + \frac{167}{0.226} = 2404^\circ \text{ R}$$

$\Delta T = 8.85 \dot{q}_{in_{stagnation}}$ for 10-second interval

t	$\dot{q}_{in}$	$\dot{q}_{av}$	ΔT	T
-20	0	1.0	8.9	400.0
-10	2	3.0	26.5	408.9
0	4	7.0	62.0	435.4
10	10	18.0	159.0	497.4
20	26	48.0	425.0	656.4
30	70	110.0	975.0	1081.4
40	150	225.0	1990.0	2056.4
50	300			4046.0

Aluminum is considered melted at t = 44 seconds and 2404° R

For the steel inner wall of the outer shell, radiation is no longer negligible.

$$\Delta \dot{q}_{radiation} = \sigma \epsilon T_w^4 \text{ or } \Delta q_R = \left(\frac{T}{1230}\right)^R$$

For Steel

Δx, Shell thickness--feet 0.00566

Δt, Time increment--seconds 1

L_F, Heat of fusion--Btu/lb 117

$$T_{final} = 3010 + \frac{117}{0.150} = 3790^{\circ} R$$

$$T = 0.835\ \dot{q}_{in_{stagnation}}$$

t	$\dot{q}_{in}$	q_{av}	Δq_r	Δq_c	ΔT	T
44	210	217.5	-8.0	209.5	174	2060
45	225	232.5	-10.5	222.0	185	2234
46	240	247.5	-15.0	232.5	193	2419
47	255	262.5	-20.0	242.5	202	2612
48	270	277.5	-32.0	245.5	204	2814
49	285	292.5	-35.0	257.5	214	3018
50	300	307.5	-35.0	272.5	227	3232
51	315	322.5	-35.0	287.5	240	3459
52	330	337.5	-35.0	302.5	252	3699
53	345	352.5	-35.0	317.0	264	3951
54	360	367.5	-35.0	332.5	278	4215
55	375					

$\therefore$ Steel is consumed at 52 seconds.

After the steel shell melted, the core heat transfer analysis was carried out by the method shown in Fig. 12. Final results of this analysis are shown in Fig. 13 and 14.

D. RESULTS

1. Solid Steel Core

A complete summary of results is presented in Table 1. A polar projection showing the final abort areas and orbital traces is shown in Fig. 15. This figure shows that it is possible to obtain open core impacts in a remote area of the Pacific Ocean south of the equator. An even wider area is shown where the unit will burn up at altitude.

Point 5A, Fig. 15, represents the largest range that the core will achieve upon abort. In this case the unit burned at 234,700 feet. This point could be considered as being equivalent to a natural decay for either a circular or elliptical orbit.

To illustrate the results more completely, an elevation view of the thrust cutoff results is presented in Fig. 16. This plot shows that the earlier the thrust is cutoff, the shorter the range and lower the aerodynamic heating. This is as expected. This results in a lesser degree of unit burnup. Figure 16 also shows the elevation view for the 45-degree thrust tilts. In this case, a partially consumed core impacts the earth's surface along the intended course. This condition describes the maximum range for partial burnup.

From the results of Fig. 15 and 16, it can be concluded that the impact area, although large, can be maintained over water in a relatively unhabited region. On the northerly path of the first orbit, where the first inhabited regions are reached, burnup will occur safely at high altitude.

Figures 15 and 16 are concerned with failure during final stage operation. Analyses were also completed for thrust cutoff during booster operation. It was found that no core melting occurred before impact for any failure during the boost phase.

2. Cluster Core

To increase the possibility of burnup, a cluster arrangement of the core as shown by Sketch c, Fig. 3 has been investigated. By arranging the cluster so that heating will be applied to four small rather than one large unit, an increase in heating can be obtained.

The gain that can be obtained is shown in Fig. 17.

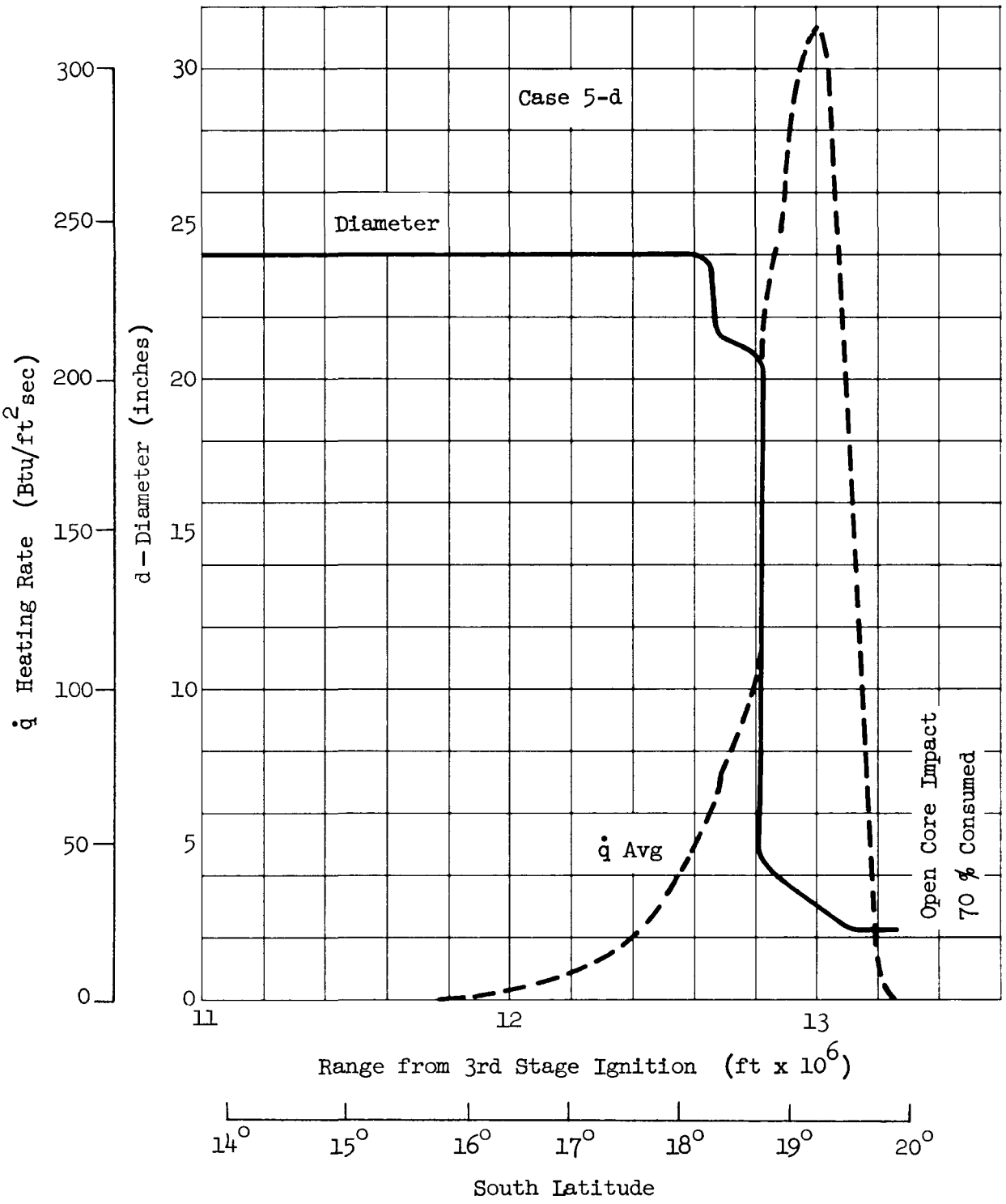

Fig. 13. Size of Re-Entry Body and Average Heating Rate vs Range

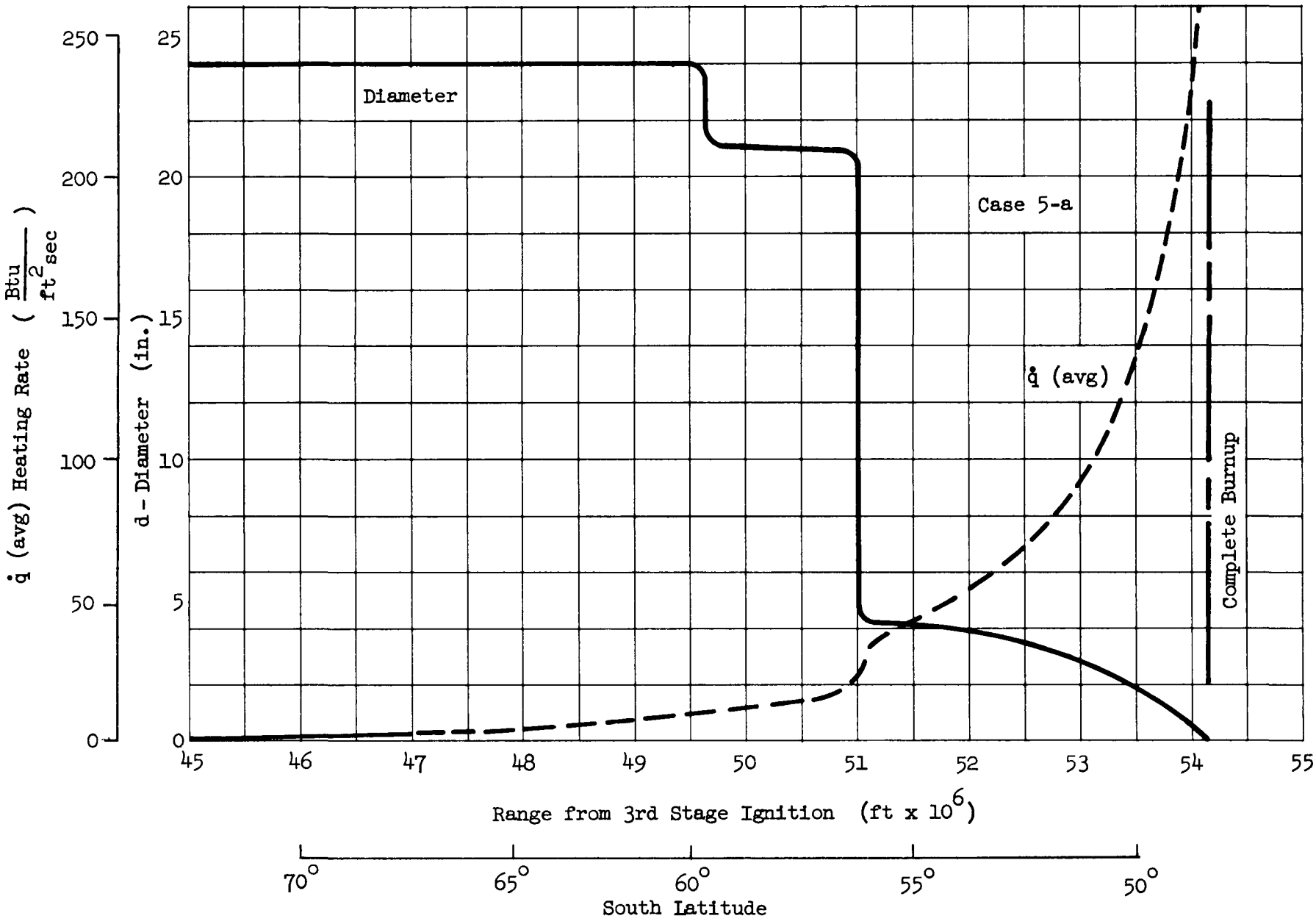

Fig. 14. Size of Re-Entry Body and Average Heating Rate vs Range

TABLE 1

End Points

	ΔV	δp	δY	φ	λ	
1a	600	5	0	--	--	Into orbit
1b	600	45	0	--	--	Into orbit
1c	600	90	0	76.9S	50.5E	Core burns out at 172,000 ft
2a	2000	5	0	--	--	Into orbit
2b	2000	45	0	53.0S	48.7E	Core burns out at 163,000 ft
2c	2000	90	0	63.9S	128.8W	Core intact at impact
3a	4000	5	0	--	--	Into orbit
3b	4000	45	0	77.0S	49.8E	Core burns out at 118,200 ft
3c	4000	90	0	46.6S	127.4W	Core intact at impact
4a	6000	5	0	--	--	Into orbit
4b	6000	45	0	88.7S	49.3E	Open core at impact 90% consumed
4c	6000	90	0	35.4S	127.5W	Core intact at impact
5a	400TCO	0	0	47.9S	49.0E	Core burns out at 234,700 ft
5b	600TCO	0	0	80.0S	127.9W	Core burns out at 179,837 ft
5c	2000TCO	0	0	36.0S	125.3W	Core burns out at 121,250 ft
5d	4000TCO	0	0	20.0S	125.1W	Open core at impact 70% consumed
5e	6000TCO	0	0			Open core at impact 28% consumed
6a	600	0	+5	--	--	Into orbit
	600	0	-5	--	--	Into orbit
6b	600	0	+45	--	--	Into orbit
	600	0	-45	--	--	Into orbit
6c	600	0	+90	64.5S	150.3W	Core burns out at 185,000 ft
	600	0	-90	64.5S	104.1W	Core burns out at 185,000 ft
7a	2000	0	+5	--	--	Into orbit
	2000	0	-5	--	--	Into orbit
7b	2000	0	+45	70.4S	140.3W	Core burns out at 178,400 ft
	2000	0	-45	70.4S	104.7W	Core burns out at 178,400 ft
7c	2000	0	+90	36.2S	135.2W	Core burns out at 105,000 ft
	2000	0	-90	36.2S	114.1W	Core burns out at 105,000 ft
8a	4000	0	+5	--	--	Into orbit
	4000	0	-5	--	--	Into orbit
8b	4000	0	+45	56.5S	141.7W	Core burns out at 169,200 ft
	4000	0	-45	56.5S	110.0W	Core burns out at 169,200 ft
8c	4000	0	+90	20.5S	135.6W	Open core at impact 80% consumed
	4000	0	-90	20.5S	113.4W	Open core at impact 80% consumed
9a	6000	0	+5	--	--	Into orbit
	6000	0	-5	--	--	Into orbit
9b	6000	0	+45	44.3S	143.3W	Core burns out at 134,960 ft
	6000	0	-45	44.3S	106.2W	Core burns out at 134,960 ft
9c	6000	0	+90	11.3S	135.7W	Open core at impact 44% consumed
	6000	0	-90	11.3S	112.5W	Open core at impact 44% consumed

φ Latitude
λ Longitude
TCO Thrust Cut Off

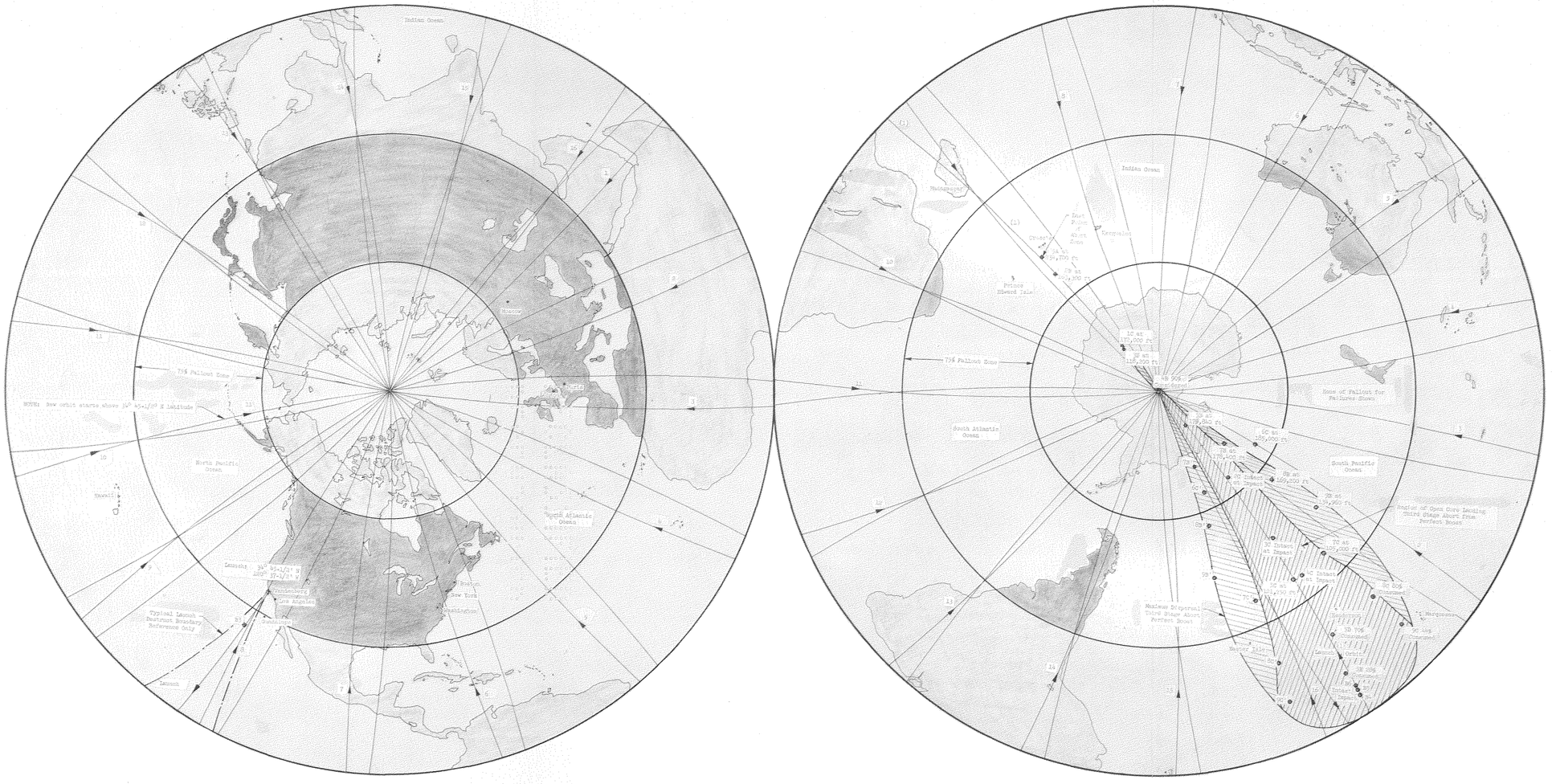

Fig. 15. Polar Projections Showing Abort Areas and Orbital Traces (zone of 75% fallout shown)

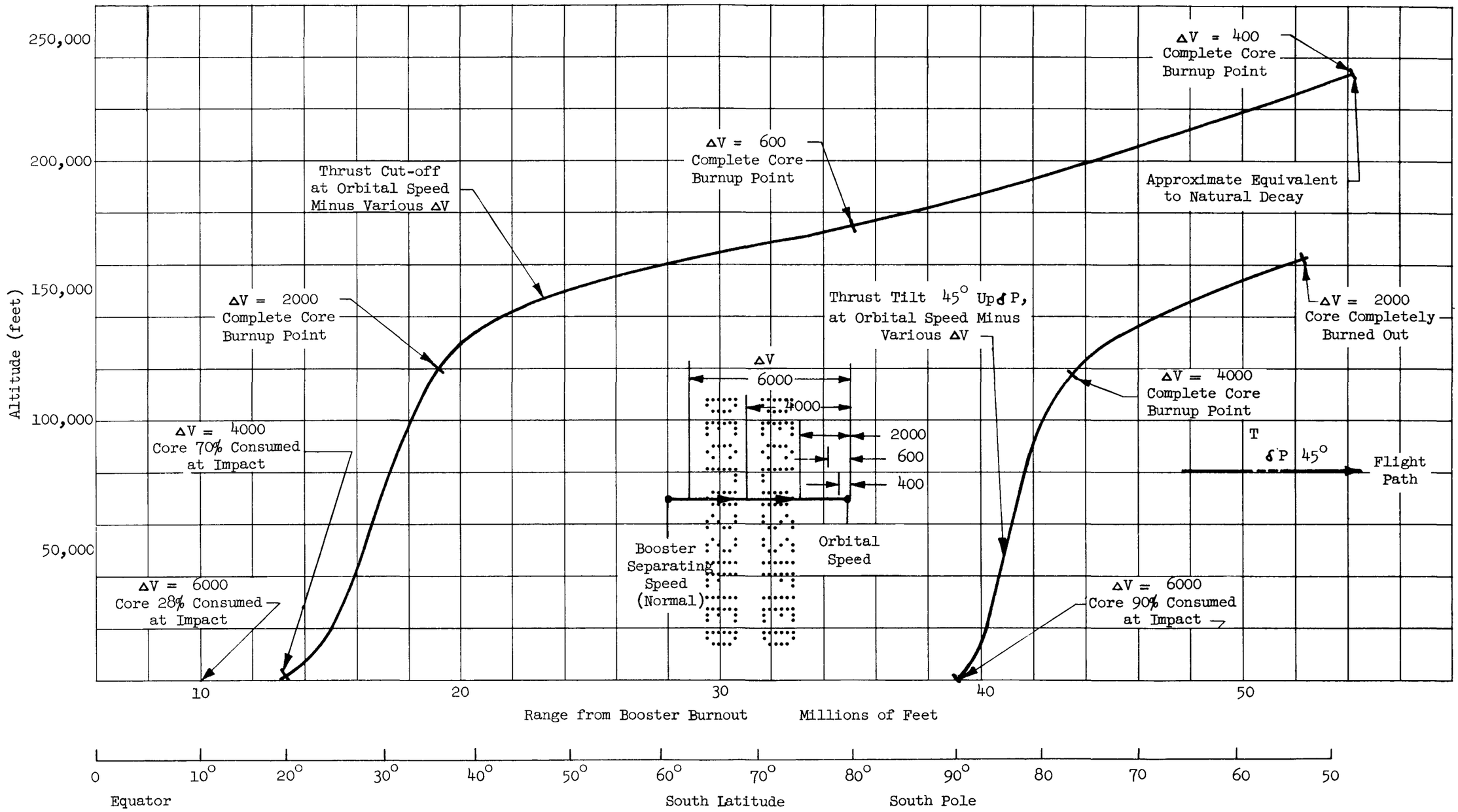

Fig. 16. Elevation Showing End Points for Various Thrust Cut-offs or Thrust Tilts During Third-Stage Operation--Standard Core

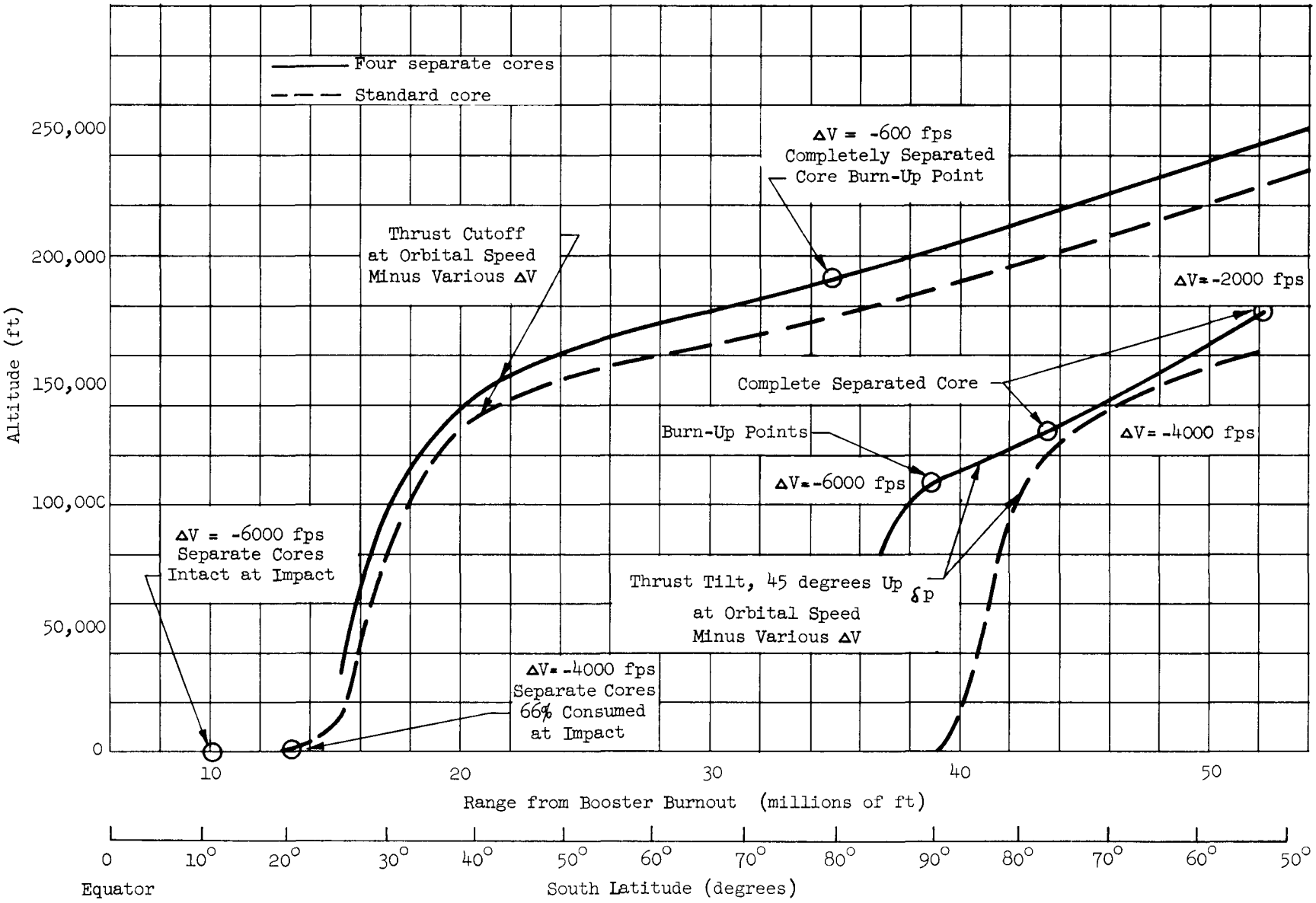

Fig. 17. Elevation Showing End Points for Various Thrust Cutoffs or Thrust Tilt During Third Stage Operation

3. Solid Molybdenum Core

To increase inpact resistance at lower temperature, molybdenum as a material for the solid core was investigated. Although molybdenum has a high melting point, it oxidizes rapidly. The Martin Company has recently conducted an extensive program on the oxidation of molybdenum loading edges for space vehicles, (Ref. 5).

This report gives the surface regression rate of molybdenum as

$$R = c\ (MFR)^K$$

where:

R = surface regression rate, in./hr

c and K constants depending upon surface temperature and pressure

MFR = mass flow rate over the surface--lb/ft^2-hr

An analysis was completed of a third-stage Abort Condition 5A using molybdenum in place of steel as a core material. Results of this study are shown in Fig. 18. This figure indicates that the molybdenum core will not completely melt before impact. Thus, radioactive diffusion can occur at low altitudes or at the earth's surface. Since Condition 5A approximately represents the natural decay condition, it becomes apparent that a molybdenum core in this configuration is not desirable from an aerodynamic burnup consideration. Other configurations which will burnup more rapidly are under study.

4. Conclusions

From the results of this study it can be concluded that:

(1) A solid steel or superalloy core configuration for a Task 2 thermoelectric generator, when launched in a southerly polar orbit from Vandenburg Air Force Base, will burn up at altitudes above 100,000 feet in a natural decay from orbit.

(2) Core impact in remote areas of the South Pacific with despersion of radioactive material at low altitudes can occur when vehicle launch faults occur during powered operation of the final stage.

(3) Improvements in burnup characteristics can be obtained by modifying the core configuration to a frangible cluster arrangement.

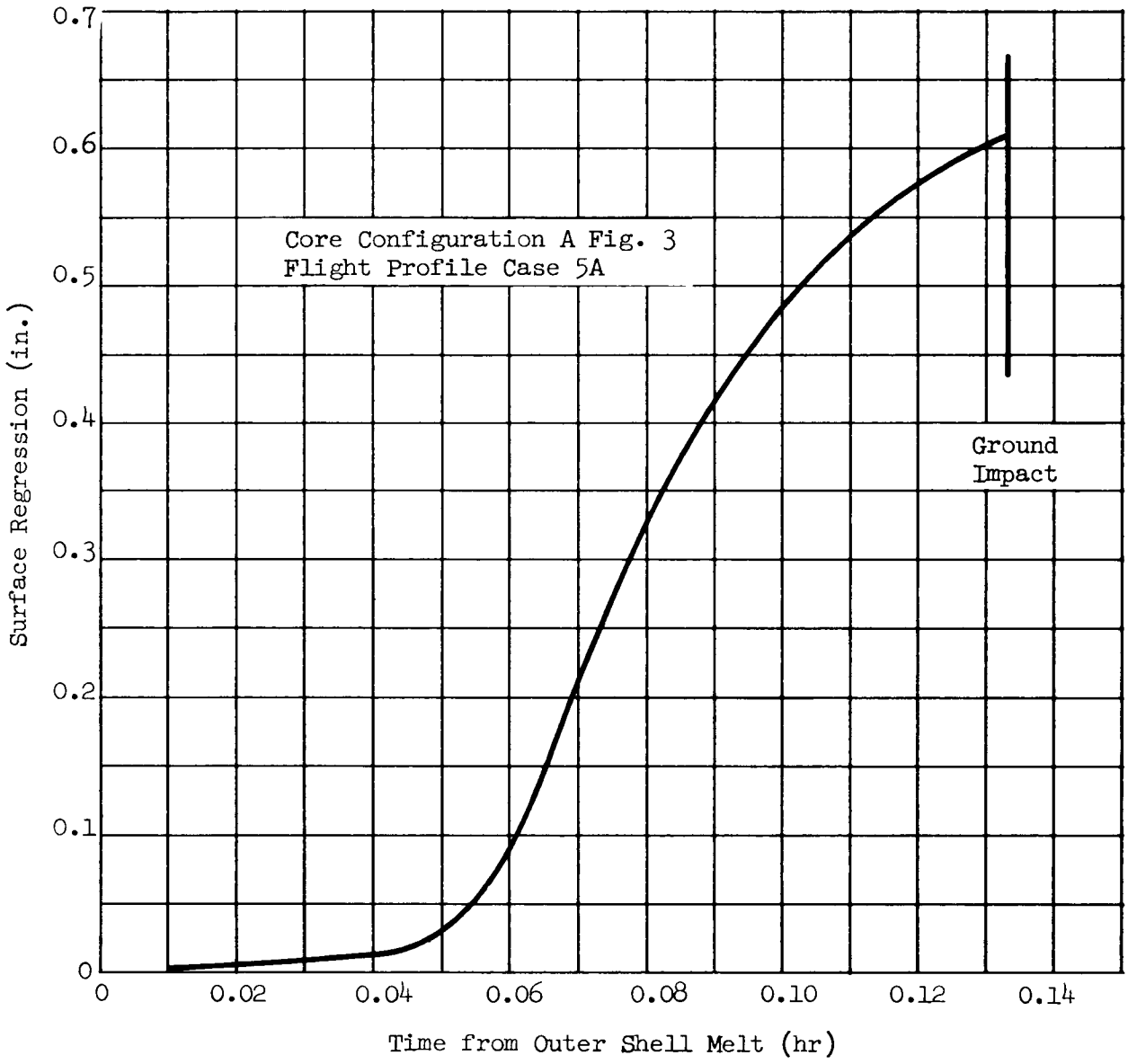

Fig. 18. Regression of Molybdenum Core Surface

(4) Use of molybdenum as a core material is detrimental to aerodynamic burnup.

(5) Assumption concerning the heat transfer model, including a correction for the satellite structure, could modify the results somewhat. However, it is not believed these are of sufficient size to change the general conclusion of the report.

REFERENCES

1. "Customer Utilization Report General N Stage Two-Dimensional Powered Trajectory", Problem No. 90-000-0-007 Martin-Baltimore Digital Unit.

2. "Basic Three-Dimensional Trajectory", Problem No. 000-0-7-028, Martin-Baltimore Digital Unit.

3. "Equation for MRBM Three-Dimensional Trajectory", Problem Digital Program No. 90-041-0-001, IDC to Digital Unit from W. H. Foy, Martin-Baltimore.

4. "Ablation Digital Program", Problem No. PG04, Martin Orlando Digital Unit-(Martin-Baltimore Program No. 021-0-F-006).

5. "Effect of Temperature, Pressure and Mass Flow on the Oxidation of Molybdenum", Charles Wilke, Martin-Baltimore, ER 10643-2, January 1960.